Ultrasound influence on I–V–T characteristics of silicon Schottky barrier structure

O. Ya. Olikh,[a] K. V. Voytenko, and R. M. Burbelo
Faculty of Physics, Taras Shevchenko National University of Kyiv, Kyiv 01601, Ukraine

(Received 19 November 2014; accepted 14 January 2015; published online 30 January 2015)

The influence of ultrasonic loading on current-voltage characteristics has been investigated in Mo/n–n^+–Si structures in the temperature range from 130 to 330 K. The longitudinal ultrasonic waves were of 8.4 MHz in frequency and had the intensity approaching 0.3 W/cm^2. The acoustically induced reversible modification of the ideality factor and the Schottky barrier height was observed. The temperature dependence of the ultrasound effect was found to be non-monotonic and the parameters variation decreased with the temperature increase from 200 to 330 K. The obtained results have been analyzed on account of the inhomogeneous Schottky barrier model. The ultrasonic loading has been shown to increase the effective density of patches, the barrier height of the uniform region and the patches region and to broaden the patch parameter distribution. © *2015 AIP Publishing LLC*.
[http://dx.doi.org/10.1063/1.4906844]

I. INTRODUCTION

Ultrasound is known to be widely applied in semiconductor physics. In particular, ultrasonic (US) waves are used to enhance an electroluminescence[1] and a photoluminescence,[2,3] to couple a laser light into graphene plasmons,[4] to modify a polarization of laser radiation[5] and a radiative recombination kinetics in quantum wells,[6] to affect carbon nanotubes[7] and metal clusters in silicon oxide,[8,9] to manipulate by nanoparticles,[10] to correlate an electron transport in heterostructures,[11,12] and to investigate spin-orbit interactions of electrons traveling in quantum wells.[13] Besides, the set of the acoustically driven effect was observed in the barrier structure. So, the ultrasound causes a recovery[14] and an increasing in the homogeneity[15] of metal-silicon structure characteristics, an improvement of characteristics of silicon p-n junction formed by ion implantation,[16] a modification of tunneling[17,18] and generation–recombination[19,20] currents in p-n structures, as well as a variation of a thermionic emission current in Schottky structures.[21,22] These changes of the electrical properties are both residual[14–16,19,20] and reversible.[17,18,21,22]

The ultrasound ability to be an effective tool in semiconductor physics deals with an acousto-electron or US wave–defect interaction. Last one is a main reason of acoustically induced effects in non-piezoelectric semiconductors. The ultrasound–defect interaction in a silicon is investigated experimentally and theoretically (e.g., see Refs. 23–25). Unfortunately, the complete theory of acousto-defect interaction in silicon is absent. In our opinion, it is partly caused by insufficient experimental data. Really, the majority of reports dealing with acoustical effects in silicon are concerned with an applying high ultrasound power at near room temperature and with a residual modification of properties. At the same time, the works that focus on the temperature dependence of reversible acoustically induced effects are very few.

This article presents the result of experimentally investigation of the acoustic strain field influence on the electrical characteristic of the Mo/n-n^+–Si structure in wide temperature range. Namely, the ultrasound influence on current value, Schottky barrier height (SBH), ideality factor was under consideration. Ultrasound has been found to result the reversible characteristic variation, i.e., parameters relax after US loading. The findings are discussed by using model of the inhomogeneous metal–semiconductor contact. The investigation would provide not only better understanding of US wave–defect interaction but could also facilitate the development of acoustically controlled devices.

II. EXPERIMENTAL AND CALCULATION DETAILS

The samples used in our experiments were 0.2 μm thick n–Si:P epitaxial layer on 250 μm thick n^+–Si:Sb substrate. The substrate N_s and epi-layer N_d carrier concentration were $4.2 \cdot 10^{22}$ m^{-3} and $7.25 \cdot 10^{21}$ m^{-3}, respectively. The square of molybdenum Schottky contact fabricated on the epi-layer surface was 7×7 mm^2.

The forward current-voltage (I–V) characteristics of the samples both with and without US loading were measured in the temperature range from 130 to 330 K. In case of US loading, the longitudinal waves excited in the samples were 8.4 MHz in frequency and had the intensity of $W_{US} < 0.3$ W/cm^2. The US loading parameters were caused by following reasons. Firstly, an acoustic wave with a frequency in the range of 1–30 MHz is able to affect defects in silicon.[14,19,20,23,26] Secondly, ultrasound with $W_{US} \geq 0.5$ W/cm^2 can lead to an unreversible modification of silicon structures.[19,20,26,27] In addition, it was reported previously[6,18,22,23,28] that a characteristic time of change in the silicon structure parameters under the ultrasound action did not exceed $2 \cdot 10^3$ s. Therefore, the I–V characteristics were measured in an hour after the US loading start.

In order to avoid the effect of piezoelectric field on I–V characteristics, the piezoelectric cell was shielded and metal

[a]Electronic mail: olikh@univ.kiev.ua

buffer was used—see Fig. 1. The sample temperature was controlled by differential copper-constantan thermocouple.

The linear and non-linear fitting were done by using the least-squares method and the method of modified artificial bee colony,[29] respectively.

III. RESULTS AND DISCUSSION

Fig. 2 shows the *I–V–T* characteristics that were measured without US loading. It can be seen that the additional current component is observed at low temperatures. The *I–V* characteristics of this additional component are affected considerably by a series resistance. Whereas semi-log *I–V* plots at high temperatures are close to a linear. Therefore, the following expression can be used to fit the *I–V* characteristic:

$$I = I_H + I_L = I_{0,H}\left[\exp\left(\frac{qV}{n_H kT}\right) - 1\right] + I_{0,L}\left[\exp\left(\frac{q(V - IR_S)}{n_L kT}\right) - 1\right], \quad (1)$$

where I_H and I_L are the high temperature current component (HTCC) and low temperature current component (LTCC), respectively, $I_{0,H}$ and $I_{0,L}$ represent the saturation current and n_H and n_L represent the ideality factor of HTCC and LTCC, respectively. The fitting results are shown in Fig. 2.

The *I–V* characteristics of structure with US loading was similar, but the current amplification was observed—see inset in Fig. 3. Below the ultrasound influence on each current component and their possible mechanisms are discussed separately.

A. High temperature current

The saturation current I_0 across an ideal Schottky barrier, based on the thermionic emission (TE) theory, is given by the relation[30]

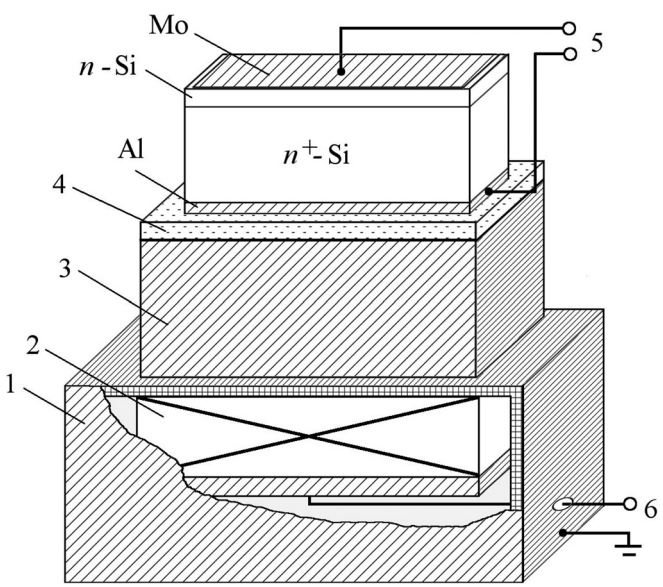

FIG. 1. Schematic of the ultrasonic loading. 1—electric shield (Al); 2—piezoelectric transducer ($LiNbO_3$); 3—buffer (Al) 4—dielectric layer (mica); 5 and 6—contact to *I–V* measure and to ultrasound excitate, respectively.

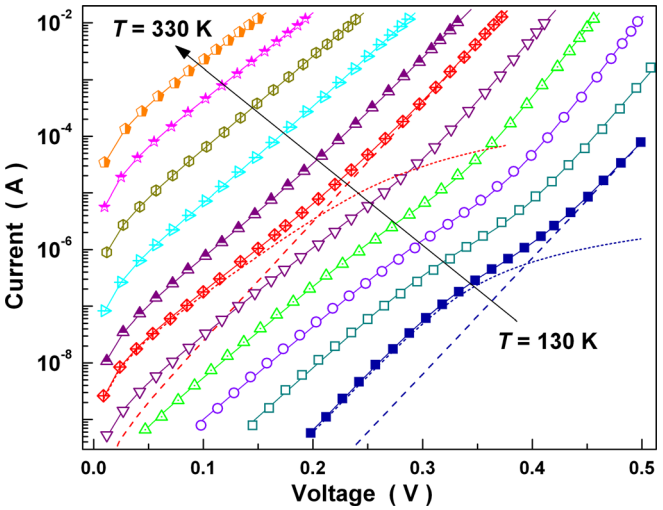

FIG. 2. *I–V* characteristics of Mo/*n*–Si Schottky structures measured at 20 K intervals from 130 to 330 K. The solid lines are the fitted curves using Eq. (1). The dashed and dotted lines are the high temperature and the low temperature current components, respectively.

$$I_0 = AA^* T^2 \exp(-q\Phi_b/kT), \quad (2)$$

where A is the diode area, A^* is the effective Richardson constant (112 A $cm^{-2}K^{-2}$ for *n*–Si (Ref. 31)), Φ_b is zero bias barrier height.

The temperature dependences of HTCC barrier height $\Phi_{b,H}$, calculated by using Eq. (2), are shown in Fig. 3. It can be seen that the $\Phi_{b,H}$ decreases under the action of ultrasound. Fig. 4 shows the dependences of SBH variation $\Delta\Phi_{b,H} = \Phi_{b,HUS} - \Phi_{b,H0}$, where $\Phi_{b,HUS}$ and $\Phi_{b,H0}$ are the barrier height at the same temperature with and without US loading, respectively.

It has been found that (i) the barrier height variation under ultrasound action has been a non-monotonic function of temperature; (ii) the maximum decrease of the SBH has

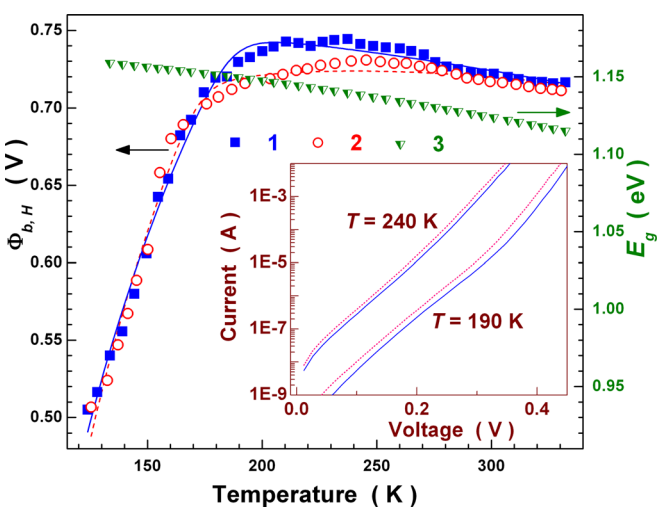

FIG. 3. Temperature dependences of silicon band gap (3) and zero bias HTCC barrier height of the Mo/*n*–Si Schottky structures with (2) and without (1) US loading. The lines are the fitted curves using Eq. (12). W_{US}, W/cm^2: 0 (1, solid line), 0.17 (2, dashed line). Inset: Two examples of *I–V* characteristics measured at the same temperature and with (dotted lines) and without (solid lines) US loading.

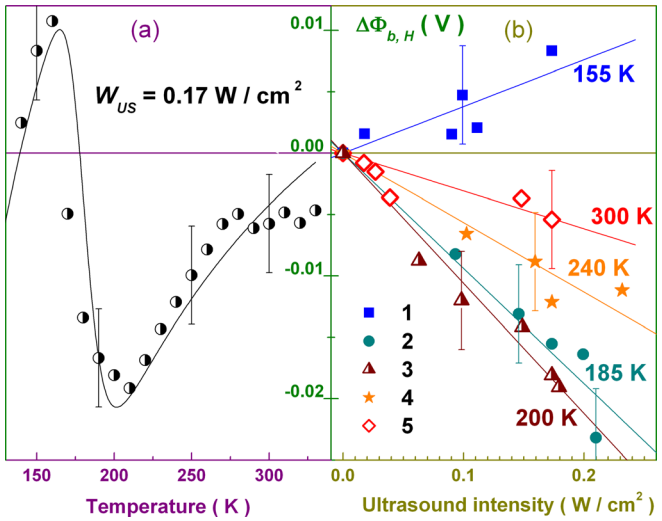

FIG. 4. Dependences of the acoustically induced HTCC barrier height variation on the temperature (a) and on the ultrasound intensity (b). The marks are the experimental results, the line in (a) is a difference between fitted curves in Fig. 3, the lines in (b) are the linear fitting. T, K: 155 (1), 185 (2), 200 (3), 240 (4), 300 (5).

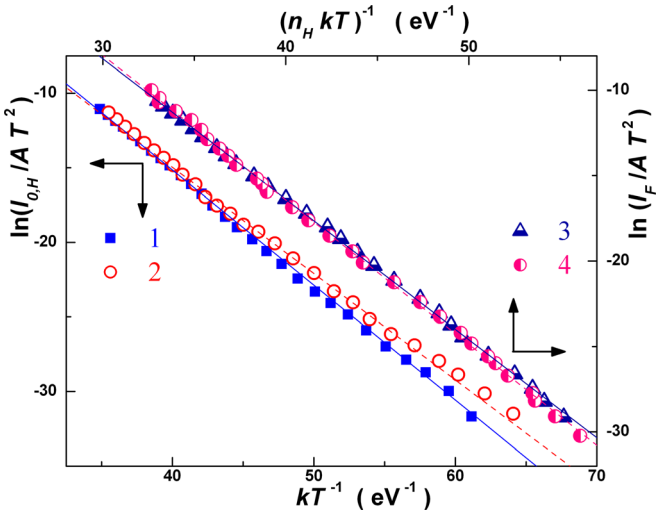

FIG. 5. Richardson (1, 2) and modified Richardson (3, 4) plots for the Mo/n–Si Schottky structures with (2, 4) and without (1, 3) US loading in the temperature range of 200–330 K. The marks are the experimental results, the lines are the linear fitting. W_{US}, W/cm^2: 0 (1, 3), 0.17 (2, 4).

approached 22 mV and has been observed at ~210 K; the US influence efficiency fells off with a temperature increasing; (iii) the SBH variation amplitude increases with the ultrasound intensity increasing and the dependences at each temperature are close to a linear. In order to better understand the possible causes of US influence, the charge transport mechanisms in the samples under study must be analyzed.

It is predicted theoretically[30] and observed experimentally,[32,33] that, in the case of homogeneous Schottky contact, the SBH decreases with temperature increase in the way similar to semiconductor band gap E_g. Fig. 2 presents also the temperature dependence of silicon E_g calculated using the Varshni equation[34]

$$E_g(T) = E_g(0) - 7.021 \cdot 10^{-4} T^2/(T + 1108), \qquad (3)$$

where $E_g(0) = 1.169$ eV is a band gap at $T = 0$ K. The observed $\Phi_{b,H}$ dependences are close to $E_g(T)$ at a temperature greater 200 K. In addition, in the case of homogeneous contact, A^* can be obtained by using the Richardson plot[30,31]

$$\ln\left(\frac{I_0}{A T^2}\right) = \ln A^* - \frac{q\Phi_b}{kT}. \qquad (4)$$

Fig. 5 (curves 1 and 2) shows the Richardson plot for HTCC in the temperature range of 200–330 K. The presented dependences are close to a linear, but the calculated from y-axis intercept of the plot A^* are found to be 1060 A cm^{-2}K^{-2} and 65 A cm^{-2}K^{-2} for structure without and with US loading, respectively. These values are not in reasonable agreement with the known value of 112 A cm^{-2}K^{-2}.

Such behavior of Richardson plot can be attributed to the bias and temperature dependence of the SBH and ideality factor, which arises due to a metal-semiconductor contact inhomogeneity.[35,36] On the other hand, the flat band condition is used to eliminate the influence of lateral inhomogeneity.[36–38] The flat-band saturation current I_F and the flat-band SBH $\Phi_{b,F}$ can be calculated from the experimental n, Φ_b and I_0 according to[36–38]

$$I_F = I_0 \exp\left[\frac{qV_n(n-1)}{nkT}\right], \qquad (5)$$

$$\Phi_{b,F} = n\Phi_b - (n-1)V_n, \qquad (6)$$

where $V_n = (kT/q)\ln(N_C/N_d)$ is the bulk potential, N_C is the effective density of states in the conduction band. Furthermore, the temperature dependence of the flat band SBH can be expressed as

$$\Phi_{b,F}(T) = \Phi_{b,F}(0) + \alpha T, \qquad (7)$$

where $\Phi_{b,F}(0)$ is the flat band barrier height extrapolated to $T = 0$ K, and α is its temperature coefficient. A plot of $\Phi_{b,F}$ for HTCC as a function of the temperature is shown in Fig. 6. In Fig. 6, the fitting of $\Phi_{b,F}(T)$ data in Eq. (7) yields $\Phi_{b,F}(0)$ and α that are listed in Table I.

According to Rhoderick and Williams,[30] the flat band barrier height can be expressed as

$$q\Phi_{b,F} = \theta(\phi_m - \chi_s) + (1-\theta)(E_g - \phi_0), \qquad (8)$$

where $\theta = [1 + (qD_s\delta)/(\varepsilon_0\varepsilon_i)]^{-1}$, ϕ_m is the metal work function, χ_s is the electron affinity of the semiconductor (4.05 eV for Si), ϕ_0 is the neutral level of the interface states, D_s is the interface state density, δ and ε_i are the thickness and permittivity of the oxide interface layer. Equation (8) does not take into account the barrier image-force lowering. Mo work function depends on a crystallographic plane as well as on a manufacturing condition and ranging from 4.53 to 4.95 eV for Mo/Si contacts.[39] Therefore, $\Phi_{b,F}$ tends to the Schottky-Mott limit $q\Phi^{SM}_{b,F} = \phi_m - \chi_s = (0.48 \div 0.90)$ eV as $D_s \to 0$ and to the Badeen limit $q\Phi^{B}_{b,F} = E_g - \phi_0$ as $D_s \to \infty$. The determinated values are within theoretical range.

In the flat band case, the modified Richardson plot is used

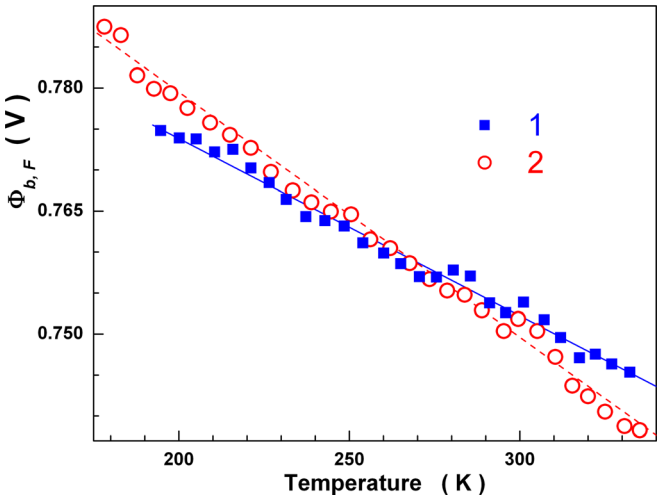

FIG. 6. Temperature dependence of the flat band barrier height for the Mo/*n*–Si Schottky structures with (2) and without (1) US loading in the temperature range of 200–330 K. The marks are the experimental results, the lines are the linear fitting. W_{US}, W/cm^2: 0 (1), 0.17 (2).

$$\ln\left(\frac{I_F}{AT^2}\right) = \ln A^*_{mod} - \frac{q\Phi_{b,F}(0)}{nkT}, \tag{9}$$

where modified Richardson constant A^*_{mod} is related to A^* by

$$A^* = A^*_{mod}\exp(q\alpha/k). \tag{10}$$

Fig. 5 (curves 3 and 4) shows the modified Richardson plots for HTCC in the temperature range of 200–330 K. $\Phi_{b,F}(0)$ and A^*_{mod} have been determined from this figure by fitting according to Eq. (9) and then A^* was calculated by using Eq. (10). The obtained values are listed in Table I. What we want to stress is that (i) the value of A^* is closer to known value and expectedly does not depend on US loading; (ii) zero temperature flat band barrier increases under ultrasound action. In our opinion, this increase is caused by the ϕ_0 lowering (the interface states charge magnification) under the ultrasound action.

Besides, the discrepancy of data obtained from Richardson plot and modified Richardson plot as well as the dependence of $\Phi_{b,H}$ in the whole temperature range of 130–330 K (Fig. 3) is reason to use inhomogeneous Schottky barrier concept. It is generally now accepted that the interfacial inhomogeneous surface is better represented as a uniform region with a random array of different patches, each of varying barrier height and area. According to the Tung's theory,[40,41] the distribution of the patch parameter γ can be described with a Gaussian function ($\gamma = 3(R_p^2\Delta/4)^{1/3}$ where R_p is the patch size and Δ is the patch barrier lowering). In this case, the relationship between Φ_b obtained from *I–V* characteristic and $1/T$ should follow a straight line[41–43]

$$\Phi_b = \overline{\Phi}_b - \frac{q\sigma_\Phi^2}{2kT}, \tag{11}$$

where mean value $\overline{\Phi}_b$ is the barrier height of a uniform region (outside patches) and standard deviation $\sigma_\Phi = \sigma_\gamma(V_{bb}/\eta)^{1/3}$, σ_γ is the γ standard deviation, $V_{bb} = \overline{\Phi}_b - V_n$, $\eta = \varepsilon_s\varepsilon_0/qN_d$, ε_s is the permittivity of the semiconductor (11.7 for Si).

However, the experimental relation on Φ_b versus $1/T$ is not simply a straight line in the whole temperature range frequently.[44–49] And it is found that the Schottky contact inhomogeneity can be described by a double-Gaussian distribution. According to this model, the barrier height can be expressed as[47–49]

$$\Phi_b = -\frac{kT}{q}\ln\left[\rho_1\exp\left(-\frac{q\overline{\Phi}_{b,1}}{kT} + \frac{q^2\sigma_{\Phi,1}^2}{2k^2T^2}\right) + \rho_2\exp\left(-\frac{q\overline{\Phi}_{b,2}}{kT} + \frac{q^2\sigma_{\Phi,2}^2}{2k^2T^2}\right)\right], \tag{12}$$

where ρ_1, $\rho_2 = 1 - \rho_1$, $\sigma_{\Phi,1}$, $\sigma_{\Phi,2}$, $\overline{\Phi}_{b,1}$ and $\overline{\Phi}_{b,2}$ are the weight, standard deviation, and mean value of two Gaussian functions, respectively.

In our experiments $\Phi_{b,H}$ versus $1/T$ does not show a simple linear relationship in the temperature range of 130–330 K. We suppose that the temperature dependence of $\overline{\Phi}_{b,i}$ follows an Eq. (3) and use Eq. (12) to fit the experimental data. The ρ_1, $\sigma_{\Phi,1}$, $\sigma_{\Phi,2}$ and zero temperature mean values $\overline{\Phi}_{b,1}(0)$ and $\overline{\Phi}_{b,2}(0)$ are taken as the fittings parameters and the results are shown in Table I and as the lines in Fig. 3. The difference between curves fitted $\Phi_{b,H}(T)$ of structure with and without US loading is shown as the line in Fig. 4(a). The good agreement of the experimental data with the fitting curves is observed.

According to Jiang *et al.*,[49] the Gaussian distribution with a little contribute (the ρ value) is caused by patches that deal with the incomplete and inhomogeneous diffusion of metal atoms. Therefore, $\overline{\Phi}_{b,2}$ and $\sigma_{\Phi,2}$ can be attributed at these defects. The $\overline{\Phi}_{b,2}$ value indicates that the large interface state density and the low neutral level are inherent in that sort of patches—see Eq. (8). At the same time, $\overline{\Phi}_{b,1}$ deals with uniform region and $\sigma_{\Phi,1}$ can be attributed at other nature patches (surface roughness, an uneven doping profile, crystal defects, etc.[50]). Rhoderick and Williams[30] showed that the barrier height was reduced from the flat band value by an amount which was proportional to the maximum

TABLE I. Extracted parameters for the Mo/*n*–Si Schottky structures with and without ultrasonic loading.

W_{US} (W/cm^2)	0	0.17
α (mV/K)	−0.22±0.02	−0.30±0.02
$\Phi_{b,F}(0)$ (mV), Fig. 6	817 ± 4	839 ± 5
$\Phi_{b,F}(0)$ (mV), Fig. 5	821 ± 4	845 ± 5
A^* (A cm^{-2}K^{-2})	116 ± 5	111 ± 5
ρ_1	0.9995	0.998
ρ_2	$0.5\cdot10^{-3}$	$2\cdot10^{-3}$
$\sigma_{\Phi,1}$ (mV)	18 ± 2	48 ± 4
$\sigma_{\Phi,2}$ (mV)	118 ± 5	127 ± 5
$\overline{\Phi}_{b,1}(0)$ (mV)	775 ± 8	809 ± 8
$\overline{\Phi}_{b,2}(0)$ (mV)	1070 ± 50	1170 ± 50
$T_{0,H}$ (K)	14 ± 1	18 ± 1
$T_{0,L}$ (K)	130 ± 5	143 ± 5
γ (10^{-5} m$^{2/3}$V$^{1/3}$)	2.7 ± 0.1	2.5 ± 0.1
C_p (10^5 m^{-2})	2.2 ± 0.4	21 ± 3

electric field in the semiconductor. The extracted relation $\Phi_{b,F} > \overline{\Phi}_{b,1}$ is relevant to the predicted tendency.

As it is shown in Table I, both the SBH mean value and the SBH standard deviation are increased by ultrasound action. It is known[30] that $\overline{\Phi}_b(0)$ a real Schottky contact is determined by interface defects. In our opinion, the reversible SBH increase is caused by the recharge or configuration rebuild of interface defects in the ultrasound strain field, which can be responsible for an energy level shift. Such acoustically induced effects were also reported previously.[51,52] In our opinion, the widen distribution of γ (the σ_Φ increasing) deals with the inequality of the acoustic influence on the patches with a different parameter.

In Fig. 7, the temperature dependence of the HTCC ideality factor is shown. The acoustically induced increasing of n has been observed in the temperature range 180–250 K. The US influence efficiency fell off with the temperature increase—see Fig. 7, inset.

The temperature dependence of the ideality factor is often described as follows:

$$n = 1 + T_0/T. \tag{13}$$

We use Eq. (13) by taking T_0 as fitting parameter to fit the experimental data in the temperature range of 200–330 K. The results are shown in Fig. 7 (the lines) and in Table I (the $T_{0,H}$ values). In case of the inhomogeneous contact, T_0 can be expressed as[43] $T_0 = q\sigma_\Phi^2/(3kV_{bb})$. Therefore, the revealed increasing of $T_{0,H}$ under the ultrasound action agrees qualitatively with the acoustically induced σ_Φ increasing.

B. Low temperature current

We use Eq. (2) to calculate the temperature dependence of the LTCC barrier height $\Phi_{b,L}$, and the results are shown in Fig. 8(a). The dependences of absolute SBH variation $\Delta\Phi_{b,L}$ under the ultrasound action are shown in Fig. 8(b). Fig. 8(b) shows that the barrier height increasing at small ultrasound intensity and at low temperature whereas the $\Phi_{b,L}$ lowering is observed at high temperature or at high ultrasound intensity. Such non-monotonic dependences anticipate two competing mechanisms of the ultrasound influence on $\Phi_{b,L}$.

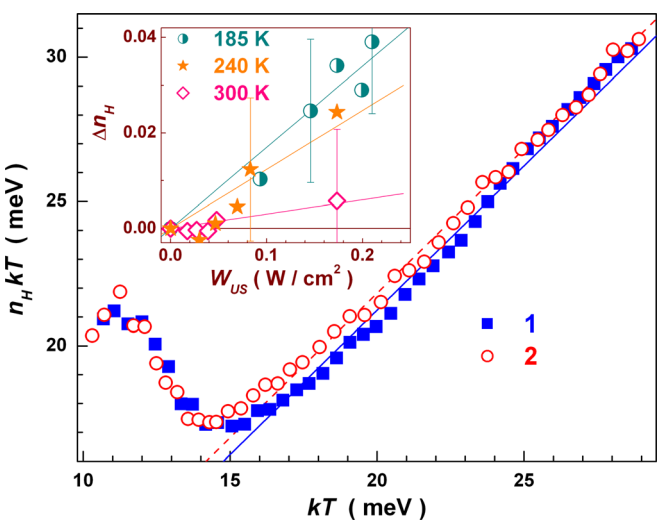

FIG. 7. Plot of $n_H kT$ as a function of kT for the Mo/n–Si Schottky structures with (2) and without (1) US loading. The marks are the experimental results, the lines are the fitted curves using Eq. (13) in the temperature range of 200–330 K. W_{US}, W/cm^2: 0 (1), 0.17 (2). Inset: the dependences of the acoustically induced ideality factor variation on the ultrasound intensity. The lines are the linear fitting.

The double bumps within the semi-log I–V characteristics, where the diode can seemingly be characterised as two diodes with parallel conduction paths, are interpreted by interface inhomogeneity too. According to the Tung's theory,[40,41] at low temperatures, the current preferentially flow through the few barriers with the lowest barrier height at small bias and the two components of current may be deconvoluted. In this case, the high value of the ideality factor of a small bias component is expected. The experimental values of n_L were changed from 2 (at 130 K) to 1.55 (at 230 K) and we used Eq. (13) to fit the data in the temperature range of 130–230 K. The fitting parameters $T_{0,L}$ are listed in Table I. In addition, the Ohmic effect may be significant for a small bias component.[40,41] It is shown[50] that the series resistance effects should become more dominant with the temperature decrease, which has been observed in our experiments (Fig. 2). In our opinion, it is evidence that the LTCC deals with the current flowing through patches.

Tung[40] showed that the saturation current of a small bias component may be simplistically written down as

$$I_0 = AA^* T^2 \frac{4C_p \pi \gamma \eta^{2/3} kT}{9V_{bb}^{2/3} q} \times \exp\left\{-\frac{q\left[\overline{\Phi}_b - \gamma(V_{bb}/\eta)^{1/3}\right]}{kT}\right\}, \tag{14}$$

where C_p is the density of patches. It follows from Eqs. (2) and (14) that

$$\Phi_{b,L} = \overline{\Phi}_b - \frac{\gamma V_{bb}^{1/3}}{\eta^{1/3}} - \frac{kT}{q}\ln\left(\frac{4C_p \pi \gamma \eta^{2/3} kT}{9V_{bb}^{2/3} q}\right). \tag{15}$$

We suppose that the $\overline{\Phi}_b$ temperature dependence follows an Eq. (3) and zero temperature $\overline{\Phi}_b$ is equal $\overline{\Phi}_{b,1}(0)$. Then we use Eq. (15) by taking γ and C_p as fitting parameters to fit the experimental temperature dependence $\Phi_{b,L}$. The results are shown in Fig. 8 and in Table I.

The carried out estimation showed that the C_p value was about 10 times as many as before US loading. In our opinion, misfit dislocations may be patches in structure under investigation and the increasing of effective density as well as the effective R_p deals with the patch oscillation in the acoustic field. On the other hand, the γ has decreased due to an ultrasound action. This is evidence of the patch barrier height increase (the Δ reduction). Thus, the interface potential is smoothed in the field of the ultrasonically induced deformation. Such reversible effects were reported previously for CdHgTe.[53] Vlasenko *et al.*[53] assumed that the point defects localized at (or near) the extended defects absorbing the ultrasound were transferred to the crystal matrix and caused the extremums in the potential relief to flatten.

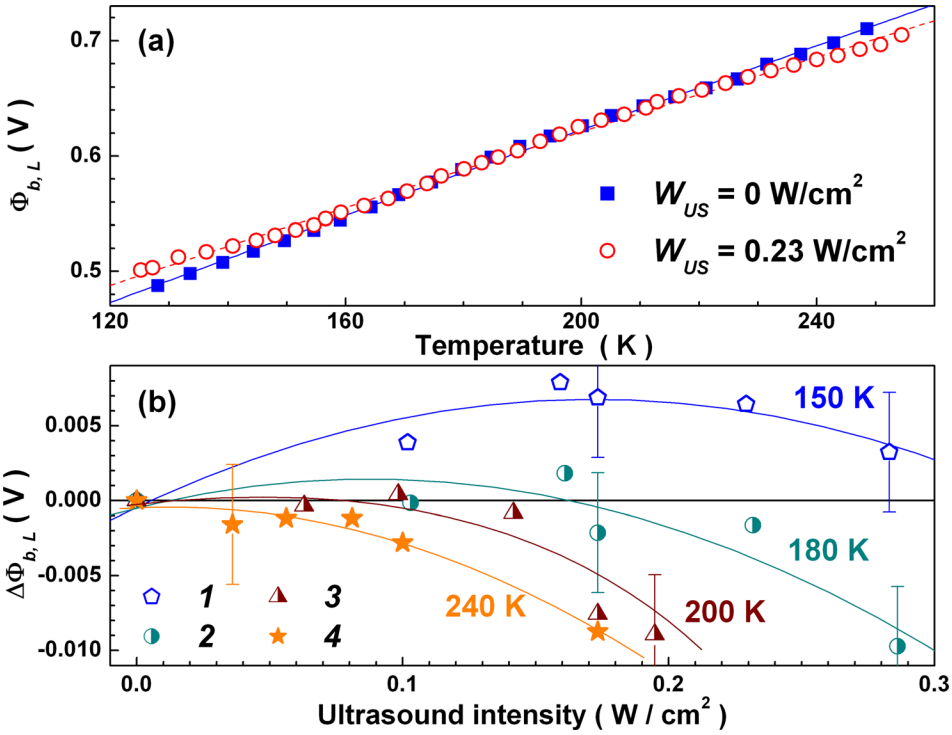

FIG. 8. (a) Temperature dependences of LTCC barrier height of the Schottky structures with and without US loading. The lines are the fitted curves using Eq. (15). (b) Dependences of the acoustically induced barrier height variation on the ultrasound intensity. T, K: 150 (1), 180 (2), 200 (3), 240 (4).

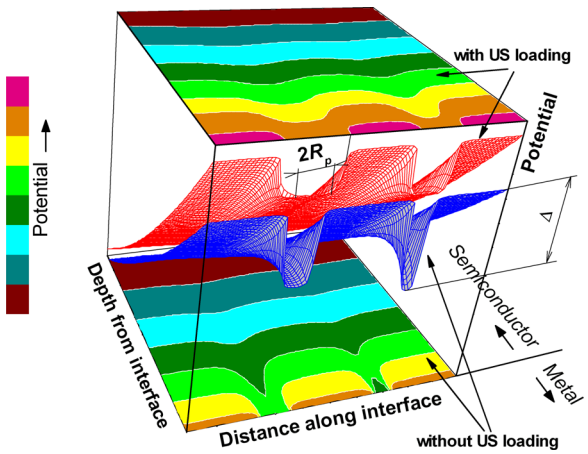

FIG. 9. Schematic conduction band diagram, showing the difference between cases with (the top surface and the top contour plot) and without (the bottom surface and the bottom contour plot) US loading. The presence of two patches is supposed. Equation (1.5.3) of Tung's model[41] was used for the potential calculation.

The patch barrier height increase can be a reason of LTCC arise at low temperature. At the same time, the dislocations are released from stoppers and patches density grows more effectively with the increasing of both temperature and acoustic strain. As a result, the effect of the patch barrier height raise is compensated and the $\Phi_{b,L}$ decrease—see Fig. 8(b).

The main features of the ultrasound action (the barrier height of the uniform region increases, the patches potential smoothing) are illustrated by Fig. 9.

IV. CONCLUSION

The experimental investigation of ultrasound influence on the electric properties of Mo/n-n^+-Si Schottky barrier structure has been carried out in the temperature range from 130 to 330 K. The investigation has revealed the acoustically induced reversible modification of the ideality factor and the Schottky barrier height. The ultrasonic waves have been shown to affect most effective at temperatures of 200–240 K. It has been found that model on inhomogeneous Schottky barrier concept is required for the current flow analysis. The analysis has shown that under the ultrasound action both barrier height of the uniform region and of the patches region increases, the patch parameter distribution broadens and the effective density of patches rises. It has been shown that the observed effects can be accounted for by the acoustically induced both oscillation of patch and recharging or configuration rebuild of interface defects. Thus, ultrasound can be an effective tool for controlling metal-semiconductor structure characteristics.

[1]W. Wang, F. Huang, Y. Xia, and A. Wang, J. Lumin. **128**, 199 (2008).
[2]A. El-Bahar, S. Stolyarova, A. Chack, R. Weil, R. Beserman, and Y. Nemirovsky, Phys. Status Solidi A **197**, 340 (2003).
[3]E. Zobov, M. Zobov, F. Gabibov, I. Kamilov, F. Manyakhin, and E. Naimi, Semiconductors **42**, 277 (2008).
[4]J. Schiefele, J. Pedros, F. Sols, F. Calle, and F. Guinea, Phys. Rev. Lett. **111**, 237405 (2013).
[5]L. Kulakova, V. Gorelov, A. Lutetskiy, and N. S. Averkiev, Solid State Commun. **152**, 1690 (2012).
[6]I. Ostrovskii, O. Korotchenkov, O. Olikh, A. Podolyan, R. Chupryna, and M. Torres-Cisneros, J. Opt. A: Pure Appl. Opt. **3**, S82 (2001).
[7]S. Pandey, U. N. Maiti, K. Palanisamy, P. Nikolaev, and S. Arepalli, Appl. Phys. Lett. **104**, 233902 (2014).
[8]A. Romanyuk, V. Spassov, and V. Melnik, J. Appl. Phys. **99**, 034314 (2006).
[9]A. Romanyuk, P. Oelhafen, R. Kurps, and V. Melnik, Appl. Phys. Lett. **90**, 013118 (2007).
[10]B. Raeymaekers, C. Pantea, and D. N. Sinha, J. Appl. Phys. **109**, 014317 (2011).
[11]S. Buyukkose, B. Vratzov, J. van der Veen, P. V. Santos, and W. G. van der Wiel, Appl. Phys. Lett. **102**, 013112 (2013).
[12]J.-H. He, J. Gao, and H.-Z. Guo, Appl. Phys. Lett. **97**, 122107 (2010).

[13]H. Sanada, T. Sogawa, H. Gotoh, K. Onomitsu, M. Kohda, J. Nitta, and P. Santos, Phys. Rev. Lett. **106**, 216602 (2011).
[14]A. Gorb, O. Korotchenkov, O. Olikh, and A. Podolian, IEEE Trans. Nucl. Sci. **57**, 1632 (2010).
[15]O. Olikh and T. Pinchuk, Tech. Phys. Lett. **32**, 517 (2006).
[16]V. Melnik, Y. Olikh, V. Popov, B. Romanyuk, Y. Goltvyanskii, and A. Evtukh, Mater. Sci. Eng., B **124–125**, 327 (2005).
[17]A. Sukach and V. Teterkin, Tech. Phys. Lett. **35**, 514 (2009).
[18]O. Olikh, Semiconductors **45**, 798 (2011).
[19]A. Davletova and S. Z. Karazhanov, J. Phys. Chem. Solids **70**, 989 (2009).
[20]A. Davletova and S. Z. Karazhanov, J. Phys. D: Appl. Phys. **41**, 165107 (2008).
[21]O. Olikh, Semiconductors **47**, 987 (2013).
[22]O. Olikh, Ultrasonics **56**, 545 (2015).
[23]S. S. Ostapenko and R. E. Bell, J. Appl. Phys. **77**, 5458 (1995).
[24]F. K. Mirzade, Semiconductors **40**, 262 (2006).
[25]R. Peleshchak, O. Kuzyk, and O. Dankiv, Condens. Matter Phys. **17**, 23601 (2014).
[26]I. G. Pashaev, Semiconductors **48**, 1391 (2014).
[27]S. I. Vlasov, A. V. Ovsyannikov, and B. N. Zaveryukhin, Tech. Phys. Lett. **35**, 312 (2009).
[28]Y. Olikh and M. Tymochko, Tech. Phys. Lett. **37**, 37 (2011).
[29]N. Karaboga, S. Kockanat, and H. Dogan, Appl. Intell. **38**, 279 (2013).
[30]E. H. Rhoderick and R. H. Williams, *Metal Semiconductor Contacts*, 2nd ed. (Clarendon Press, Oxford, 1988).
[31]D. K. Schroder, *Semiconductor Material and Device Characterization*, 3rd ed. (John Wiley & Sons, New Jersey, 2006).
[32]M. Aboelfotoh, J. Appl. Phys. **66**, 262 (1989).
[33]S. Zhua, R. L. V. Meirhaeghea, C. Detaverniera, G.-P. Rub, B.-Z. Lib, and F. Cardon, Solid State Commun. **112**, 611 (1999).
[34]J. Munguia, J.-M. Bluet, O. Marty, G. Bremond, M. Mermoux, and D. Rouchon, Appl. Phys. Lett. **100**, 102107 (2012).
[35]K. Sarpatwari, S. E. Mohney, and O. O. Awadelkarim, J. Appl. Phys. **109**, 014510 (2011).
[36]D. A. Aldemir, A. Kokce, and A. F. Ozdemir, Microelectron. Eng. **98**, 6 (2012).
[37]M. H. Unewisse and J. W. V. Storey, J. Appl. Phys. **73**, 3873 (1993).
[38]H. Korkut, N. Yildirim, and A. Turut, Microelectron. Eng. **86**, 111 (2009).
[39]R. Lin, Q. Lu, P. Ranade, T.-J. King, and C. Hu, IEEE Electron Device Lett. **23**, 49 (2002).
[40]R. T. Tung, Phys. Rev. B **45**, 13509 (1992).
[41]R. T. Tung, Mater. Sci. Eng., R **35**, 1 (2001).
[42]F. Iucolano, F. Roccaforte, F. Giannazzo, and V. Raineri, J. Appl. Phys. **102**, 113701 (2007).
[43]F. Iucolano, F. Roccaforte, F. Giannazzo, and V. Raineri, Appl. Phys. Lett. **90**, 092119 (2007).
[44]A. Kumar, K. Asokan, V. Kumar, and R. Singh, J. Appl. Phys. **112**, 024507 (2012).
[45]O. Y. Olikh, IEEE Trans. Nucl. Sci. **60**, 394 (2013).
[46]I. Tascioglu, U. Aydemir, and S. Altindal, J. Appl. Phys. **108**, 064506 (2010).
[47]Y.-L. Jiang, G.-P. Ru, F. Lu, X.-P. Qu, B.-Z. Li, W. Li, and A.-Z. Li, Chin. Phys. Lett. **19**, 553 (2002).
[48]N. Yildirima, A. Turut, and V. Turut, Microelectron. Eng. **87**, 2225 (2010).
[49]Y.-L. Jiang, G.-P. Ru, F. Lu, X.-P. Qu, B.-Z. Li, and S. Yang, J. Appl. Phys. **93**, 866 (2003).
[50]P. M. Gammon, A. Perez-Tomas, V. A. Shah, O. Vavasour, E. Donchev, J. S. Pang, M. Myronov, C. A. Fisher, M. R. Jennings, D. R. Leadley, and P. A. Mawby, J. Appl. Phys. **114**, 223704 (2013).
[51]O. Y. Olikh, Semiconductors **43**, 745 (2009).
[52]O. Korotchenkov and H. Grimmliss, Phys. Rev. B **52**, 14598 (1995).
[53]A. I. Vlasenko, Y. M. Olikh, and R. K. Savkina, Semiconductors **34**, 644 (2000).